Caveolin-1 Loss of Function Accelerates Glucose Transporter 4 and Insulin Receptor Degradation in 3T3-L1 Adipocytes

Elena González-Muñoz, Carmen López-Iglesias, Maria Calvo, Manuel Palacín, Antonio Zorzano, and Marta Camps

Departament de Bioquímica i Biologia Molecular (E.G.-M., M.P., A.Z., M.C.), Facultat de Biologia, Universitat de Barcelona, Institute for Research in Biomedicine (IRB Barcelona) (E.G.-M., M.P., A.Z.), and Unitat de Reconeixement Molecular (C.L.-I.), Serveis Cientifico-Tècnics, Universitat de Barcelona, 08028 Barcelona, Spain; and Unitat de Microscòpia Confocal (M.C.), Serveis Cientifico-Tècnics, Universitat de Barcelona, Facultat de Medicina, and Centro de Investigación Biomédica en Red de Diabetes y Enfermedades Metabólicas (CIBERDEM) (A.Z., M.C.), CIBERDEM Asociadas, Mallorca 183, 08036 Barcelona, Spain

Caveolae are a specialized type of lipid rafts that are stabilized by oligomers of caveolin protein. Caveolae are particularly enriched in adipocytes. Here we analyzed the effects of caveolin-1 knockdown and caveolae ablation on adipocyte function. To this end, we obtained several multiclonal mouse 3T3-L1 cell lines with a reduced expression of caveolin-1 (95% reduction) by a small interfering RNA approach using lentiviral vectors. Control cell lines were obtained by lentiviral infection with lentiviral vectors encoding appropriate scrambled RNAs. Caveolin-1 knockdown adipocytes showed a drastic reduction in the number of caveolae (95% decrease) and cholera toxin labeling was reorganized in dynamic plasma membrane microdomains. Caveolin-1 depletion caused a specific decrease in glucose transporter 4 (GLUT4) and insulin receptor protein levels. This reduction was not the result of a generalized defect in adipocyte differentiation or altered gene expression but was explained by faster degradation of these proteins. Caveolin-1 knockdown adipocytes showed reductions in insulin-stimulated glucose transport, insulin-triggered GLUT4 recruitment to the cell surface, and insulin receptor activation. In all, our data indicate that caveolin-1 loss of function reduces maximal insulin response through lowered stability and diminished expression of insulin receptors and GLUT4. We propose that caveolin-1/caveolae control insulin action in adipose cells. **(*Endocrinology* 150: 3493–3502, 2009)**

Lipid rafts are lateral assemblies of sphingolipids and cholesterol that form a separate liquid-ordered phase in the liquid-disordered matrix of the lipid bilayer (1). Lipid rafts function as platforms with which distinct classes of proteins are associated, such as glycosylphosphatidylinositol-anchored proteins, transmembrane proteins, and diacylated proteins.

Caveolae are a specialized type of lipid raft that appear in the plasma membrane (PM) as 50- to 100-nm flask-shaped invaginations. Caveolae function has been widely debated and has been implicated in membrane traffic, signal transduction, substrate transport, and endocytosis (2). Caveolae are present in most cell types but are particularly abundant in adipocytes, where they account for 30% of the PM surface area (3). In adipocytes, caveolin-1 isoform is responsible for caveolae formation (4).

Adipose tissue plays a critical role in energy homeostasis in higher organisms. It serves as the main site for energy storage in the form of triglycerides and also contributes to systemic glucose and lipid metabolism via its function as an endocrine organ. In unstimulated basal adipocytes, less than 5% of glucose transporter 4 (GLUT4) is in the PM. Insulin regulates glucose transport in adipose tissue by increasing the amount of GLUT4 in the PM. After insulin removal, GLUT4 is rapidly internalized from the PM and is effectively sequestered within the cell, thus decreasing adipocyte glucose uptake.

ISSN Print 0013-7227 ISSN Online 1945-7170
Printed in U.S.A.

doi: 10.1210/en.2008-1520 Received October 29, 2008. Accepted April 21, 2009.
First Published Online April 30, 2009

Abbreviations: CTxB, cholera toxin B subunit; FAT, fatty acid transporter; FRAP, fluorescence recovery after photobleaching; GFP, green fluorescent protein; GLUT4, glucose transporter 4; GM1, monosialotetrahexosylganglioside; IR, insulin receptor; IRS-1, IR substrate 1; KD, knockdown; KO, knockout; PKCζ, protein kinase Cζ; PM, plasma membrane; PML, PM lawn; siRNA, small interference RNA.

The characterization of the caveolin-1 knockout mouse phenotype associated, for the first time, caveolin-1/caveolae with lipid homeostasis and obesity. Lisanti's group (5) showed that despite being hyperphagic, adult caveolin-1-null mice were lean and resistant to diet-induced obesity and exhibited reduced fat pads compared with wild-type littermates. Recently, it has been reported that rare caveolin-1 frameshift mutations are associated with atypical lipodystrophy and hypertriglyceridemia (6, 7). Furthermore, *caveolin-1* gene expression is up-regulated in visceral and sc white adipose tissue in obese nondiabetic or type 2 patients compared with lean controls (8).

Recently, the groups led by Pilch and Parton (9, 10) have shown that cavin/polymerase I and transcript release factor, a caveolae-associated protein, is an essential component of caveolae. Mice lacking cavin have no morphologically detectable caveolae in any cell type examined and have markedly diminished protein expression of all three caveolin isoforms. *Cavin* knockout mice have higher circulating triglyceride levels, reduced adipose tissue mass, glucose intolerance, and hyperinsulinemia (11).

A role for caveolin-1 in insulin signaling and its potential involvement in diabetes has been proposed (12). Young caveolin-1 knockout mice fed a normal diet show a blunted response to an insulin tolerance test (13). In further studies, it has been demonstrated that caveolin-1 interacts with insulin receptor (IR) and enhances insulin-mediated phosphorylation of IR substrate 1 (IRS-1) (14, 15). Caveolae integrity is required for IR signaling, which leads to GLUT4 translocation to the PM (4, 4, 16–19).

Caveoale have been related to GLUT4 endocytosis. There are data documenting the mediation of GLUT4 endocytosis by two pathways, one clathrin dependent and another one dependent on cholesterol-enriched domains in adipocytes (20–23).

However, to analyze the function of caveolae in insulin-stimulated GLUT4 translocation and GLUT4 endocytosis, cholesterol-aggregating or -depleting reagents, such as filipin, nystatin, and β-methylcyclodextrin, have been used (17–19, 21, 24, 25). These reagents do not discriminate between lateral noncaveolar lipid rafts and invaginated caveolae, because both types of lipid microdomains are sensitive to cholesterol depletion.

To analyze the effect of specifically disrupting caveolae microdomains, we repressed caveolin-1 protein in 3T3-L1 adipocytes using the RNA interference method. Our results show that caveolin-1 participates in GLUT4 and IR protein stability, thus altering maximal insulin response stimulating glucose transport of caveolin-1 knockdown (KD) adipocytes.

Materials and Methods

Antibodies

The following antibodies were used: anti-caveolin-1, anti-caveolin-2, anti-flotillin-1, anti-IR β-subunit, and anti-phosphotyrosine (PY20) from Transduction Laboratories (Lexington, KY); anti-GLUT4 (OSCRX) (26), anti-p85 subunit of phosphatidylinositol-3-kinase, and anti-perilipin from Upstate Biotechnology (Lake Placid, NY); anti-acetyl-coenzyme A-carboxylase, IRS-1, Akt, phospho-Akt(Ser473), phospho-Akt(Thr308), phospho-MAPKp44/p42 (Thr202/Tyr204), GSK-3, phospho-GSK3(Ser21), PKCζ, and phospho-PKCζ(Thr410) from Cell Signaling Technology (Beverly, MA); anti-c-Cbl from Santa Cruz Biotechnology (Santa Cruz, CA); anti-GLUT1 from Alpha Diagnostic International Inc. (San Antonio, TX); anti-FATP1 and anti-FATP4 supplied by Dr. A. Stahl (Palo Alto Medical Foundation, Palo Alto, CA); anti-FAT/CD36 supplied by Dr. W. Stremmel (Ruprechts-Karls-University, Heidelberg, Germany); anti-LPL supplied by Dr. J. Peinado (Barcelona University, Barcelona, Spain); and anti-SSAO supplied by Dr. S. Jalkanen (Turku University, Turku, Finland). Alexa555-CtxB, LysoTracker Red, and Alexa555-human transferrin were from Molecular Probes (Invitrogen, Barcelona, Spain).

3T3-L1 cell culture

3T3-L1 fibroblasts (CCL 92.1; American Type Culture Collection, Manassas, VA) were induced to differentiate into adipocytes essentially as described (27) Cells were used 8–11 d after initiation of differentiation.

Design and subcloning of small interfering RNA (siRNA)

On the basis of the established characteristics of siRNA-targeting constructs described by Dr. D. Trono (www.tronolab.com), we designed a caveolin-1 siRNA duplex corresponding to bases 301-319 from the open reading frame of the murine caveolin-1 mRNA: 5′-AACCAGAAGGGACACACAG-3′. The scrambled sequence used as a negative control for siRNA activity was 5′-AAAACCGAAGACAGACGGC-3′.

siRNA sequence templates were inserted into human H1 promoter containing pLVTHM lentiviral vector, as described by Dr. D. Trono (http://tronolab.epfl.ch). Each hairpin consisted of a *Mlu*I site, a 19-nucleotide sense sequence, a short spacer (TTCAAGAGA), a 19-nucleotide antisense sequence, five thymidines (a STOP signal for RNA polymerase III), and a *Cla*I site. We constructed a siRNA for mouse caveolin-1 (sicav1) and a control siRNA (scrambled) that does not affect any murine protein using oligo pairs (sense and antisense strands are *underlined*; *italics* indicate loop): sicav1, ACGCGTCCCCAACCAGAAGGGACACACAG*TTCAAGAGA*CTGTGTGTCCCTTCTGGTTTTTTTGGAAATCGAT, and scrambled, ACGCGTCCCCAAAACCGAAGACAGACGG*CTTCAAGAGA*GCCGTCTGTCTTCGGTTTTTTTTTGGAAATCGAT.

Lentivirus production and infection of 3T3-L1 preadipocytes

All HIV-1-derived lentiviral constructs (pLVTHM transfer vector, pCMVΔ8,74 helper packaging construct and pMD2G vector encoding for envelope protein) were kindly provided by Dr. D. Trono from the Ecole Polytechnique Federale de Lausanne (Switzerland). The pLVTHM allows siRNA expression under H1 promoter, and it also contains a green fluorescent protein (GFP) expression cassette. Lentiviruses encoding scrambled and caveolin-1 siRNA were produced by triple transient transfection of HEK 293T (28). 3T3-L1 preadipocytes grown on six-well plates were transduced at 60 multiplicity of infection, and cells were amplified during 5–7 d. Transduced cells (GFP-positive) expressing similar levels of GFP protein were then sorted with a MoFlo flow cytometer (Dako Diagnostics SA, Barcelona, Spain; Submmit version 3.1 software), obtaining 95–99% GFP-positive cells.

Triton X-100 and sucrose density gradient fractionation of lipid rafts/caveolae

The experiments were performed as previously described (29). For detection of glycosphingolipid monosialotetrahexosylganglioside (GM1), 10 μl of each fraction from the density gradient centrifugation were dot-blotted onto Hybond C membrane (Bio-Rad Spain, Madrid, Spain) and incubated with horseradish peroxidase-conjugated cholera toxin subunit B (Sigma-Aldrich, Madrid, Spain).

PM lawn (PML) techniques and immunofluorescence staining analysis

PML were prepared as described previously (30) and adapted for 3T3-L1 adipocytes as described previously (20). Immunofluorescence and immunogold techniques were adapted using an anti-GLUT4 polyclonal antibody (OSCRX) and an anti-caveolin-1 polyclonal antibody. For immunofluorescence staining, we used goat antirabbit-Alexa568 (Molecular Probes) as secondary antibody.

For GLUT4 colocalization studies, we incubated control and caveolin-1 KD adipocytes with 50 nM LysoTracker or with 1 μg/ml Alexa555-human transferrin for 1 h at 37 C. Cells were then fixed, and GLUT4 was immunolocalized. Quantitative colocalization analyses were performed using Huygens Essential software (IZASA SA, Madrid, Spain). Colocalization was analyzed within the entire images. The same threshold values were used for all images. Manders' M1 and M2 colocalization coefficients were calculated.

Fluorescence recovery after photobleaching (FRAP) imaging and data analysis

FRAP experiments were carried out using a Leica TCS SP5 laser scanning confocal spectral microscope (Leica Microsystems Heidelberg GmbH, Mannheim, Germany). 3T3-L1 adipocytes were incubated with 1 μg/ml Alexa555-CTxB (Molecular Probes Invitrogen) at 4 C for 30 min and washed in PBS. FRAP experiments were performed at 20 C and 5% CO_2 to reduce internalization. For visualization of Alexa555, images were acquired using ×63 PL APO glycerol immersion objective (NA 1.3), 561-nm laser line, acousto-optical beam splitter 571–650 nm, and the confocal pinhole set at 1.5 Airy units.

For FRAP experiments of Alexa555-CTxB in 3T3-L1 adipocytes, 10 single scans, prebleach, were acquired at 500-msec interval followed by 14 bleach scans (280-msec interval) at full power laser line (514 and 561 nm) using a rectangular area of 2 × 6.5 μm. Bleaching region was placed in the peripheral rim of the labeled adipocyte. In the postbleach period, 100 images were acquired at 500-msec interval followed by 140 images acquired at 1-sec intervals, time to enable fluorescence to reach equilibrium. For pre- and postbleach imaging, excitation intensity was attenuated with acousto-optical tunable filter to 3–7% of the line laser power to avoid significant photobleaching, and images were acquired at 1000 Hz (bidirectional) in a 512- × 512-pixel format, pixel size 160 × 160 nm.

Mean fluorescence intensity in regions of interest during the time series were quantified using the Image Processing Leica Confocal software. Background fluorescence was measured in a random field outside of the cells and subtracted from all measurements. A neighbor cell total fluorescence was determined for each image and compared with the initial cell fluorescence to correct for signal loss during imaging.

For each time point, the fluorescent intensity in the region of interest was background subtracted, corrected, and finally normalized (according to Ref. 31). Fitting of curves was performed with GraphPad Prism software version 3.0 (GraphPad Software, San Diego, CA) assuming a one-phase exponential (from bottom, then increase to top) equation: Y (fluorescence recovery) = bottom + (top − bottom) × [1 − exp(−KX)].

Preparation of carbon-platinum replicas of the inner cell surface

Replicas were obtained as described previously (30). For immunogold assays, replicas were not digested with household bleach; instead, they were washed in distilled water for 4 d to preserve the colloidal gold attached to the replicas (21).

Conventional transmission electron microscopy

The 3T3-L1 adipocytes were processed as described previously (21).

Oil red O staining of trigliceryides

The 3T3-L1 adipocytes were fixed with 3% paraformaldehyde for 15 min and then stained with Oil red O for 1 h followed by washing with 70% methanol and water (32).

Measure of glucose uptake and GLUT4 endocytosis

2-D-Deoxyglucose uptake measurements were performed as described previously (33).

Phosphotyrosine proteins immunoprecipitation: analysis of IR, IRS-1, and c-Cbl tyrosine phosphorylation

Control and caveolin-1 KD 3T3-L1 adipocytes were starved for 2 h in high-glucose DMEM/0.2% BSA and were then incubated for 5 min with 100 nM insulin. Cells were washed with ice-cold PBS and lysed in 1% Igepal buffer [50 mM HEPES (pH 7.4), 10 mM EDTA, 150 mM NaCl, 10 mM sodium pyrophosphate, 100 mM sodium fluoride, 1 mM sodium vanadate, and a tablet of C-complete (Roche Diagnostics, Sant Cugat, Spain) protease inhibitor cocktail]. Cell lysates (500 μg) were immunoprecipitated with anti-phosphotyrosine antibody and processed for Western blot analysis using anti-β-subunit of IR antibody, anti-IRS-1, and anti-c-Cbl antibodies.

Measurement of IR and GLUT4 turnover

Cells in a 60-mm dish were washed and incubated in methionine-free DMEM for 30 min at 37 C, followed by pulse labeling in methionine-free DMEM containing 10% dialyzed fetal bovine serum and 110 μCi/dish of [^{35}S]methionine (Perkin Elmer España, Madrid, Spain) for 12 h. The cells were washed with PBS and incubated in complete DMEM supplemented with 10% fetal bovine serum and 100 μg/ml L-methionine.

The labeled cells were washed with ice-cold PBS and lysed with 1 ml lysis buffer (150 mmol/liter NaCl; 1.0% Nonidet P-40; 0.1% sodium dodecyl sulfate; 1 mmol/liter EDTA/Na; and 50 mmol/liter Tris/Cl, pH 8.0). The lysates were immunoprecipitated with anti-GLUT4 or anti-IR antibody and analyzed as described previously (34).

Cell fractionation

Cell fractionation was performed as described previously (35).

RNA expression studies

Total RNA extraction and treatment with deoxyribonuclease I were done with Trizol reagent (Invitrogen). Total RNA from 3T3-L1 adipocytes at were kept at −80 C until further assay. RNA concentration was determined by spectrophotometry at an absorbance of 260 nm. Real-time PCR was performed from 0.1 μg total RNA from adipocyte cells, as described previously (36). Cyclophilin or aRP (acidic ribosomal protein) mRNA were assayed as controls in real-time PCR assays. The following primers were used: caveolin-1 forward AACATCTAC AAGCCCAACAACAAGG and reverse GGTTCTGCAATCACATCTTCAAAGTC, caveolin-2 forward ATGACGCCTACAGCCACCACAG and reverse GCCTAGCTT GAGATGAGAGTTGAG, perilipin forward TGCTGGATGGAgACCTC and reverse ACCGGCTCCATGCTCCA, aP2 forward TTCGATGAAAT-CACCGCAGA and reverse GGTCGACTTTCCATCCCACTT, HSL forward GGCTTACTGGGCACAGATACCT and reverse CTGAAG-GCTCTGAGTTGCTCAA, LPL forward AGG ACCCCTGAAGACAC and reverse GGCACCCAACTCTCATA, CD36 forward GATGTG-GAACCCATAACTGGATTCAC and reverse GGTCCCAGTCTCATT-TAGCCACAGTA, GLUT1 forward CCCCCGCTTCCTGCTCATC and reverse CTGCCGACCCTCTTCTTTCATC TC, cyclophilin forward CTTTGACTTGCGGGCATTTTAC and reverse AAGAACTTCAGT-GAGAGCAGAGATTACAGG, and aRP forward AAGCGCGTCCTG-GCATTGTCT and reverse CCGCAGGG GCAGCAGTGGT.

Results

Lentivirus-mediated siRNA expression efficiently blocks caveolin-1 in 3T3-L1 preadipocytes and adipocytes

To selectively knock down the expression of caveolin-1 protein in 3T3-L1 adipocytes, we obtained 3T3-L1 cell lines with a reduced expression of caveolin-1 using a pLVTHM lentiviral vector expressing a siRNA fragment for murine caveolin-1. A scrambled sequence was also used as negative control. We infected 3T3-L1 preadipocytes, as described in *Materials and Methods*. Several infections were performed to rule out artifactual phenotypes, and several 3T3-L1 cell lines expressing caveolin-1 siRNA (sicav1) or scrambled siRNA (control) were generated and analyzed.

Caveolin-1 expression in sicav1-infected 3T3-L1 preadipocytes was dramatically reduced (97%) (Fig. 1A). This decrease in expression was also detected in mature 3T3-L1 adipocytes (95% reduction) (Fig. 1B). In addition, we analyzed the abundance of caveolin-1 in the PM by immunolocalization on PML from control or caveolin-1 KD adipocytes. Data indicate that caveolin-1 was barely detectable on PM of sicav1-infected adipocytes compared with the control group (Fig. 1C).

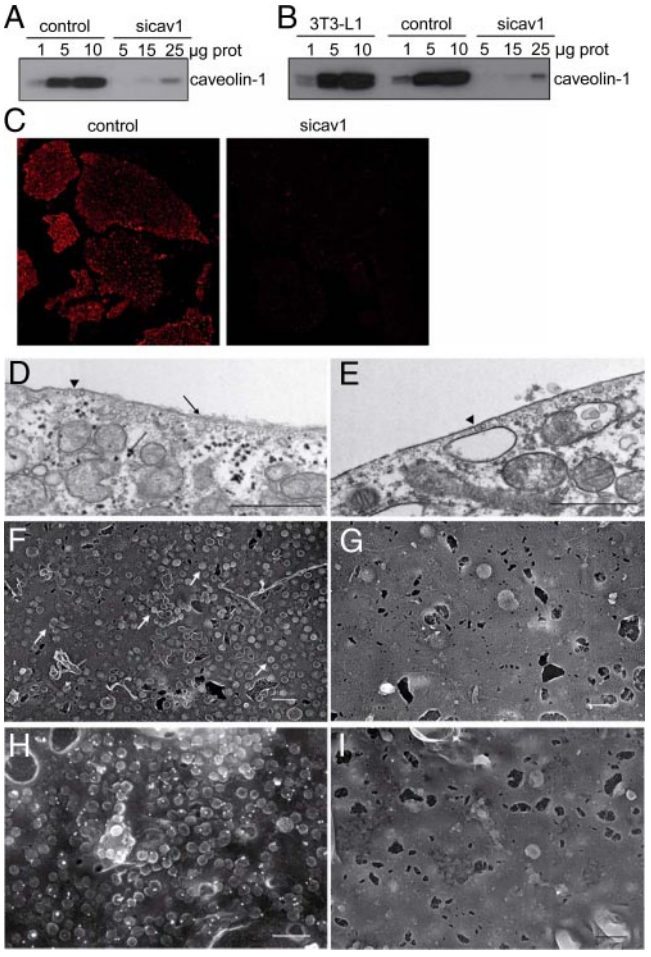

FIG. 1. siRNA mediated down-regulation of caveolin-1 expression in 3T3-L1 adipocytes and causes caveolae ablation. A, 3T3-L1 preadipocytes were infected with 60 multiplicity of infection of scrambled or caveolin-1 siRNA (sicav1) lentivirus. Infected cells were selected as explained in the *Materials and Methods* and lysed. Different quantities of protein (prot) from cell lysates were used to analyze caveolin-1 expression by PAGE and Western blot with an anti-caveolin-1 antibody. B, Different quantities of protein lysates obtained from adipocytes differentiated from scramble and sicav1 preadipocytes were analyzed as in A.The same was done with adipocytes differentiated from preadipocytes described in A and from noninfected preadipocytes (3T3-L1). C, PML were obtained from adipocytes expressing scrambled or caveolin-1 (sicav1) siRNAs as described in *Materials and Methods* and were used to immunolocalize caveolin-1. Images were obtained with a confocal microscope using Alexa568 secondary antibody. *Bar*, 25 μm. D,Transmission electron microscopy was used to visualize caveolae on the PM of ultrathin sections from D control (scrambled siRNA infected) (D) and caveolin-1 KD (caveolin-1 siRNA infected) (E) adipocytes. *Arrows* show caveolae bunches, and *arrowheads* show individual caveolae. Replicas of PML from control (F) and caveolin-1 KD (G) adipocytes obtained by freeze-drying technique were used to visualize and quantify caveolae. Caveolin-1 was immunolocalized with an anti-caveolin-1 polyclonal antibody and a 15-nm colloidal gold goat antirabbit secondary antibody on PML from control (H) and caveolin-1 KD adipocytes (I).

Caveolin-1 KD causes the ablation of caveolae in adipocytes

As a first approach, to corroborate that deficiency in caveolin-1 induces caveolae ablation, we obtained ultrathin resin sections from control and caveolin-1 KD adipocytes (Fig. 1, D and E). A smaller number of caveolae were observed in the PM of caveolin-1 KD adipocytes than in PM of control adipocytes, and in fact, the few caveolae detectable in caveolin-1 KD cells were isolated, and no caveolae bunches were shown (Fig. 1E). Caveolin-1-depleted adipocytes showed a marked reduction (80%) in cavin expression (data not shown).

Next, we characterized PML at the electron microscope level. To this end, membranes were fixed with glutaraldehyde, and after washing with water and methanol as cryoprotectant, they were rapidly frozen against a copper block cooled by liquid nitrogen. PML were then freeze-dried in a freeze-etching unit, and rotatory replicas of platinum-carbon were obtained following the Heuser and Anderson technique (30). The replicas showed inner surfaces of PM clean of cytoplasmic organelles, except for cytoskeletal elements (Fig. 1, F and G). Clathrin-coated pits and flat clathrin lattices were observed in PML from control and caveolin-1 KD adipocytes. The PM of the latter showed very few

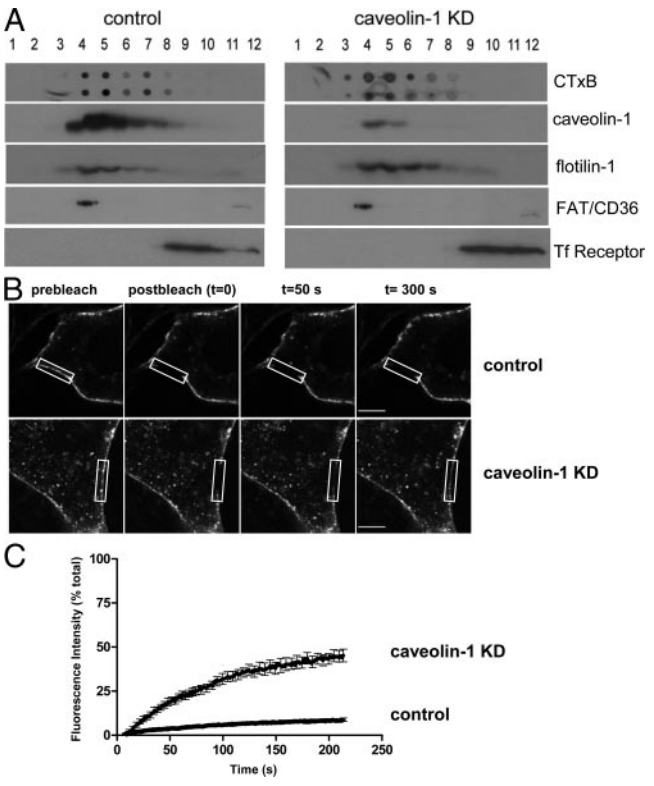

FIG. 2. Lipid raft markers in caveolin-1 KD cells are reorganized in dynamic PM microdomains. A, Control and caveolin-1 KD adipocytes were subjected to subcellular fractionation using 1% Triton X-100 extraction and ultracentrifugation in a discontinuous sucrose gradient. An aliquot of each fraction was dot-blotted and incubated with horseradish peroxidase-conjugated CTxB or resolved by SDS-PAGE and analyzed by Western blot with specific antibodies as shown. B, Selected images from a confocal FRAP experiment in control and caveolin-1 KD adipocytes labeled with Alexa555-CTxB at 20 C. *Bar*, 5 μm. C, Kinetics of recovery for Alexa555-CTxB; each *curve* shows the mean ± SEM from eight cells from a single experiment. The calculated mobile fractions were as follows: control adipocytes, 7.2 ± 0.8%; and caveolin-1 KD adipocytes, 43 ± 3.7%.

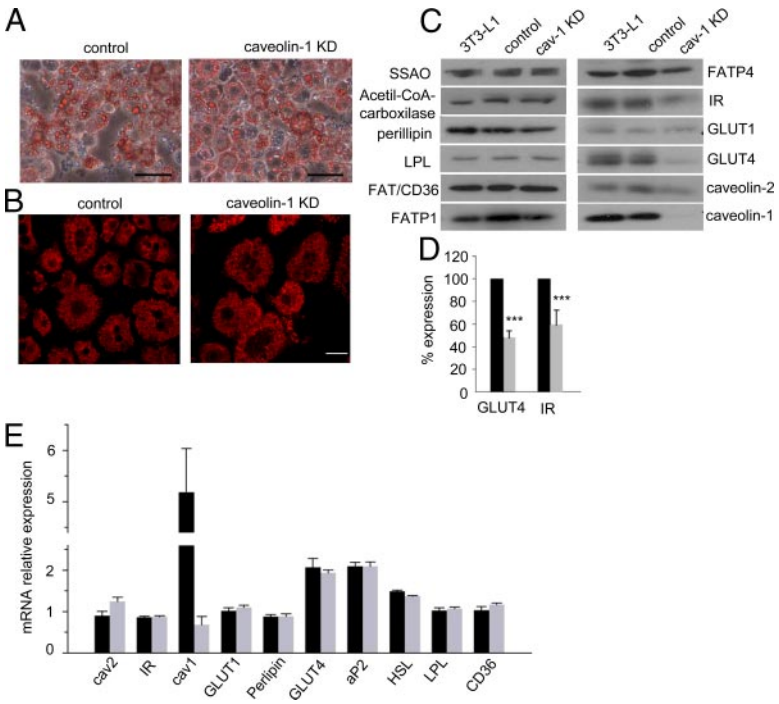

FIG. 3. Effect of caveolin-1 deficiency on adipocyte and morphology: specific repression of GLUT4 and IR proteins. A and B, Control and caveolin-1 KD adipocytes 10 d after the induction of differentiation were stained with Oil red O (A) (*bar*, 40 μm) or subjected to immunofluorescence using an anti-perilipin (B) (*bar*, 25 μm). C, 3T3-L1 adipocytes not infected (3T3-L1) or infected with scramble (control) or sicav1 lentivirus (caveolin-1 KD) on d 10 after the induction of differentiation were lysed, and 20 μg cell lysates were resolved by SDS-PAGE and analyzed by Western blot with specific antibodies, as shown. LPL, Lipoprotein lipase; SSAO, semicarbazide-sensitive amino-oxidase. D, Densitometric analyses from immunoblot data show levels of GLUT4 and IR expression in control (*black bars*) and caveolin-1 KD (*gray bars*) adipocytes. Each data point represents the mean ± SEM derived from seven independent experiments. Student's *t* test was performed between caveolin-1 KD and control cells. ***, $P \leq 0.005$. E, Control (*black bars*) and caveolin-1 KD (*gray bars*) adipocytes were lysed, and mRNA levels of several markers of mature adipocytes were measured by real-time RT-PCR as described in *Materials and Methods*.

caveolae. The number of caveolae/μm^2 ± SEM calculated from 30 micrographs of PML samples were 74.8 ± 10 and 4.06 ± 1.41 in control and caveolin-1 KD adipocytes, respectively. This observation indicates a 95% reduction in the number of caveolae in caveolin-1 KD cells, which is parallel to the global caveolin-1 abundance.

When we immunolabeled caveolin-1 on PML before freezing them (Fig. 2, C and D), in control adipocytes, caveolin-1 localized on caveolae. However, caveolin-1 was associated mostly with planar parts of the PM in caveolin-1 KD adipocytes (Fig. 1, H and I). Taken together, these results provide compelling evidence that caveolin-1 siRNA sequences block the expression of caveolin-1 protein and lead to ablation of caveolae on the cell surface. Thus, caveolae formation requires the expression of caveolin-1 in adipocytes.

Lipid raft markers in caveolin-1 KD cells are reorganized in dynamic PM microdomains

Caveolae are a subtype of lipid raft characterized by the presence of caveolin-1. Both caveolae and lipid rafts have a distinctive lipid composition, in that they are enriched in cholesterol and sphingolipids and therefore characterized by a low buoyant density, which facilitates their subcellular fractionation. On the basis of prior data, we next analyzed the abundance and distribution of lipid raft markers, such as cholera toxin B subunit (CTxB), that binds to GM1 glycosphingolipid, caveolin-1, flotillin-1, and fatty acid transporter (FAT)/CD36 in control and caveolin-1 KD adipocytes. To this end, we homogenized adipocytes at 4 C in the presence of 1% Triton X-100. This method has been widely used to isolate lipid raft fractions and preserves their structure and components (37).

GM1 and protein markers of lipid rafts (flotillin-1 and FAT/CD36) were localized in the same gradient fractions in control and caveolin-1 KD adipocytes (Fig. 2A). Transferrin receptor fractionation on sucrose gradient was used as a negative control of a protein widely described to be absent in lipid rafts/caveolae. In addition, the abundance of all these markers was similar in both cell types. The same results were obtained when we isolated lipid rafts using an extraction with sodium carbonate at pH 11 in the absence of detergents, as described previously (38) (data not shown).

We measured diffusional mobility of raft-associated lipids using FRAP experiments in control and caveolin-1 KD adipocytes labeled with Alexa555-CTxB at 20 C. In these experiments, we photobleached an area of the rim of adipocyte PM using high-intensity laser, and the diffusive exchange of photobleached CTxB with nearby unbleached molecules was then followed for 200 sec (Fig. 2, B and C). Recovery into the bleached region was higher in caveolin-1 KD adipocytes than in control adipocytes. The mean mobile fraction (Mf) values ± SEM calculated from two independent experiments (n = 14 cells) were 8 ± 0.8 and 42 ± 2.7% in control and caveolin-1 KD adipocytes, respectively. Mf reports the fraction of fluorescent molecules that were able to recover into the bleached area over the time course of the experiment.

Deficiency in caveolin-1/caveolae causes a specific repression of GLUT4 and IR proteins

Caveolae number and caveolin-1 protein expression are strongly increased during adipogenesis (3, 4). Thus, we studied the effect of caveolin-1 KD on 3T3-L1 adipocyte differentiation. No differences were detected in the morphology of differentiated adipocytes (Fig. 3A), the appearance of lipid droplets (Fig. 3B), or the triglyceride content in cell lysates (mean values expressed in nanomoles per microgram protein ± SEM were 0.42 ± 0.02 and 0.45 ± 0.05 in control and caveolin-1 KD adipocytes, respectively) in response to caveolin-1 repression. We also analyzed the expression of protein markers characteristic of mature adipocytes such as semicarbazide-sensitive amino-oxidaze, acetyl-coenzyme A-carboxylase, perilipin, lipoprotein lipase, FAT/CD36, FATP1, FATP4, IR, and GLUT4 (Fig. 3C). Most of these proteins did not undergo any changes in response to caveolin-1 repression. However, GLUT4, IR, and caveolin-2 were markedly down-regulated in caveolin-1 KD adipocytes (Fig. 3C). Caveolin-2 protein stability has been widely reported to depend on caveolin-1 expression (39, 40), and as a result, caveolin-1-defi-

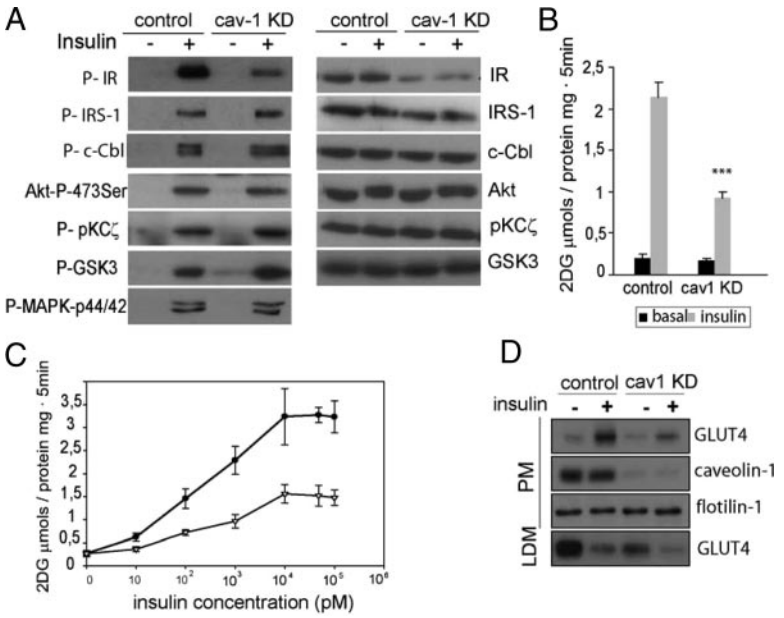

FIG. 4. Analysis of insulin pathway activation and plasma membrane GLUT4 translocation. A, Control and caveolin-1 KD adipocytes were incubated with (+) or without (−) 100 nM insulin for 5 min. Cells were lysed, and 1 mg cell extract was used for immunoprecipitation with an anti-phosphotyrosine antibody. Immunoprecipitates were blotted with anti-IRS-1 antibody (P-IRS-1), anti-c-Cbl antibody (P-c-Cbl), or anti-IR β-subunit (P-IR). Cell lysates (100 μg) were also resolved by SDS-PAGE and analyzed by Western blot using specific antibodies as shown. *Left panels* show phosphorylation of insulin signaling pathway proteins, and *right panels* show total expression of these proteins. GSK3, Glycogen synthase kinase 3; P-GSK3, phospho-GSK3; P-MAPK-p44/42, phospho-MAPK-p44/42 P-pKCζ, phospho-pKCζ. B, Control and caveolin-1 KD adipocytes were treated (*gray bars*) or not (*black bars*) with 100 nM insulin for 30 min, and glucose uptake was measured by 2-deoxy-[^{3}H]glucose (2DG) uptake in 5 min. Student's *t* test was performed between caveolin-1 KD and control cells. ***, $P \leq 0.005$. C, Control (●) and caveolin-1 KD (△) adipocytes were treated with a range of insulin concentrations (10 and 100 pM and 1, 10, 50, and 100 nM) for 30 min, and 2DG uptake was measured as in B. Graph shows the mean ± SEM derived from seven independent experiments. Two-way ANOVA indicated significant differences between the control and the caveolin-1 KD groups at $P < 0.01$. D, GLUT4 translocation to PM after insulin stimulation. Control and caveolin-1 KD adipocytes incubated in the presence (+) or absence (−) of 100 nM insulin for 30 min were subjected to subcellular fractionation as explained in *Materials and Methods*. PM (15 μg) and low-density membranes (LDM) were resolved by SDS-PAGE and analyzed by immunoblots using specific antibodies against GLUT4, caveolin-1, and flotillin-1.

cient cells also lack caveolin-2. GLUT4 and IR expression was diminished by 50 and 40%, respectively, in caveolin-1 KD adipocytes (Fig. 3D).

Real-time PCR analysis of the levels of mRNA for several genes in adipocytes revealed normal expression in caveolin-1-deficient adipocytes (Fig. 3E). These data suggest that caveolin-1 deficiency is linked to a translational or posttranslational defect for GLUT4 and IR expression.

Adipocytes deficient in caveolin-1/caveolae show reduced insulin-stimulated glucose transport

Next, we studied the activation of insulin signaling pathway by analyzing the phosphorylation of a number of intermediates described to participate in the classical phosphatidylinositol 3-kinase-dependent pathway [IRS-1, Akt, and protein kinase Cζ (PKCζ)] (41, 42) and in the caveolae-associated Cbl/TC10 pathway (c-Cbl) (16, 43). We also examined insulin activation of MAPK and glycogen synthase kinase-3. Insulin-stimulated IR tyrosine phosphorylation was lower in caveolin-1 KD adipocytes compared with control cells (Fig. 4A). Under these conditions, insulin-stimulated phosphorylation of IRS-1, Akt, PKCζ, glycogen synthase kinase-3, MAPK or c-Cbl was normal (Fig. 4A).

Measurement of 2-D-deoxy[^{3}H]glucose uptake revealed a marked reduction of insulin-stimulated glucose transport (50% reduction) in caveolin-1-deficient adipocytes compared with control cells (Fig. 4B). Under these conditions, basal glucose transport was unaltered (Fig. 4B). Reduced insulin-stimulated glucose uptake was explained by a lowered translocation of GLUT4 to the PM in adipocytes (Fig. 4D).

We also studied the insulin sensitivity of caveolin-1 KD adipocytes by measuring 2-deoxyglucose uptake at a range of insulin concentrations (Fig. 4C). Estimation of insulin EC_{50} values revealed that caveolin-1 KD cells were less insulin sensitive than control adipocytes (EC_{50} values were 0.31 and 0.71 nM in control and caveolin-1 KD adipocytes, respectively). In all, our data indicate that specific deficiency in caveolin-1/caveolae reduces IR function, and this, together with the reduced GLUT4 expression, causes insulin resistance in adipocytes, which is characterized mainly by a reduced maximal response to insulin.

Caveolin-1/caveolae deficiency reduces the half-lives of GLUT4 and IR proteins

To determine the mechanisms by which caveolin-1 deficiency caused down-regulation of IR and GLUT4, we analyzed GLUT4 and IR protein turnover in control and caveolin-1 KD adipocytes. [^{35}S]Methionine pulse-chase analysis revealed a significant increase in IR (Fig. 5A) and GLUT4 (Fig. 5B) degradation in the absence of caveolin-1. Quantification of four independent experiments was performed in cells to estimate protein half-lives. Data indicated that the half-life of IR was 6.3 h in control adipocytes and 2.7 h in caveolin-1 KD adipocytes. GLUT4 half-life was 36 and 22 h in control and caveolin-1 KD adipocytes, respectively. In all, caveolin-deficient adipocytes showed a faster degradation of IR and GLUT4 proteins.

Caveolae are not essential for GLUT4 internalization after insulin removal

Our group has reported that lipid rafts are required for GLUT4 internalization after insulin washout in adipocytes and that a substantial percentage of GLUT4 is localized in caveolae (21). In adipocytes, 30% of the PM surface are caveolae (3), so the vast majority of lipid rafts are caveolae. In caveolin-1 KD adipocytes, caveolae, but not lipid rafts, disappeared from the PM. Thus, we studied whether GLUT4 internalization, which is active after insulin removal, is affected by the lack of caveolae. GLUT4 abundance in PML was higher in insulin-treated cells than in cells in the basal state in both control and caveolin-1 KD adipocytes (Fig. 6A). As expected, PML from control adipocytes showed greater GLUT4 expression levels than caveolin-1-deficient adipocytes (Fig. 6A). Fifteen minutes after insulin removal, GLUT4 was reduced at the cell surface (Fig. 6A). However,

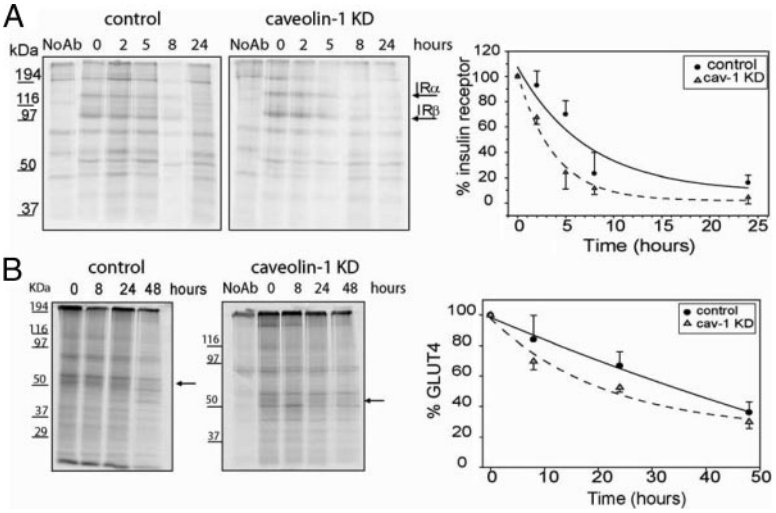

FIG. 5. IR and GLUT4 half-lives are reduced in caveolin-1-deficient adipocytes. Control and caveolin-1 KD 3T3-L1 adipocytes were pulse labeled with [^{35}S]methionine for 12 h. Adipocytes were washed and chased in fresh medium for the indicated periods. At the end of the incubation, IR (A) or GLUT4 (B) was immunoprecipitated from the cell lysates and subjected to autoradiography as described in *Materials and Methods*. A control lane immunoprecipitated without antibody (NoAb) is also shown. *Left panels* show representative autoradiogram data. *Right panels* show ^{35}S radioactivity in the IR (A) or GLUT4 (B) bands expressed as the percentage of the initial value. Results are shown as the mean ± SD (n = 4). Two-way ANOVA indicated significant differences between the control and the caveolin-1 KD groups, at $P < 0.05$.

caveolin-1 deficiency did not block the internalization of GLUT4. Fluorescence intensity of GLUT4 on PML was determined by confocal microscopy (using the fluorescence intensity/pixel area). We analyzed the decrease of GLUT4 signal on the PML of adipocytes 15 min after the removal of insulin, and we quantified a reduction of GLUT4 staining of 28 ± 5% (SEM) and 25 ± 5% (SEM) in control and caveolin-1 KD adipocytes, respectively.

To further analyze the effect of caveolae deficiency on GLUT4 internalization induced by insulin removal, we assayed the down-regulation of 2-deoxyglucose transport after insulin washout (Fig. 6B). To this end, adipocytes were initially stimulated with insulin for 30 min, washed at pH 6.0 to remove insulin, and incubated at 37 C for a range of times up to 30 min. This procedure has been previously used to shut off insulin action (33). We estimated the decrease in 2-deoxyglucose uptake and fitted the regression curve of GLUT4 internalization over time. The lack of caveolin-1 did not significantly alter this process (Fig. 6B).

To further analyze GLUT4 localization, we incubated control and caveolin-1 KD adipocytes with 50 nM LysoTracker (Fig. 6C) or with 1 μg/ml Alexa555-human transferrin (Fig. 6D) for 1 h at 37 C. Quantitative colocalization analyses were performed using Huygens Essential software (IZASA SA). Manders' colocalization coefficients were calculated; GLUT4 colocalization with transferrin was 0.335 ± 0.021 and 0.296 ± 0.026 for control and caveolin-1 KD adipocytes, respectively (differences were not significant). GLUT4 colocalization with Lysotracker was 0.041 ± 0.007 and 0.138 ± 0.0026 for control and caveolin-1 KD adipocytes, respectively. These data indicate that colocalization of GLUT4 with the lysosomal marker was increased in caveolin-1 KD adipocytes. This finding suggests that one of the pathways involved in the increased degradation of GLUT4 in the absence of caveolin-1/caveolae is lysosomal. However, when we assessed the overlap of GLUT4 and the endosomal marker transferrin receptor, we did not observe any difference between control and caveolin-1 KD adipocytes.

Discussion

In this study, we have shown that the decrease in the expression of caveolin-1 in 3T3-L1 adipocytes leads to a concomitant reduction in the number of caveolae on the PM. This effect promotes a diminished expression of IR and GLUT4 in caveolin-1 KD adipocytes, which is due to a faster degradation of these proteins and not to a defect in gene expression or adipocyte differentiation. Caveolin-1-deficient adipocytes show reductions in insulin-stimulated glucose transport, insulin-triggered GLUT4 translocation to the cell surface, and IR activation.

Caveolae and noncaveolar lipid rafts are membrane lipid microdomains with similar lipid composition (44, 45). The major difference between these two structures is the main protein component of caveolae, caveolin, which give caveolae their invaginated shape. The large abundance of caveolae in specific cell types, such as smooth muscle cells, fibroblasts, endothelial cells, and adipocytes, has motivated us to investigate the role of this structure in each cell type. The 3T3-L1 adipocytes are a cell line with major caveolae abundance in the PM. This feature corresponds with the high expression of caveolin-1 in these cells, which is notably increased during adipogenesis. Most of the methods that have been used to abolish caveolae, and therefore study their function is based on cholesterol depletion or capture, thus disturbing caveolae and lipid rafts (46). In this regard, we have analyzed the effect of specific ablation of caveolae from the PM. Lipid and protein markers of caveolae (flotillin and FAT/CD36), still remained in low-density membranes in the absence of caveolae, and their expression was not reduced as assessed by subcellular fractionation. In embryonic fibroblasts of caveolin-1 knockout (KO) mice, it has been shown that FAT/CD36 is redistributed to detergent-soluble membranes (47) in contrast to what we have described in caveolin-1 KD adipocytes.

FRAP experiments performed in control adipocytes indicated that Alexa555-CTxB-labeled membrane microdomains were highly immobile (<8%), comparable to previously reported stability of caveolin-1 in caveolae (48). The low diffusional mobility of CTxB in control adipocytes, resembling that of caveolae markers, suggests that GM1 mainly localizes in caveolae. However, in caveolin-1 KD adipocytes, devoid of caveolae, FRAP experiments showed that the mobility of Alexa555-CTxB in PM was increased (42%), suggesting that GM1 redistributed to membrane microdomains more dynamic than caveolae. This change in mobility can be produced by caveolin-1 loss; however, it cannot be ruled out that a change in lipid composition of these microdomains is also produced. We have not studied the specific order and composition properties of adipocyte membranes in the presence or absence of caveolin-1 to identify the kind of trans-

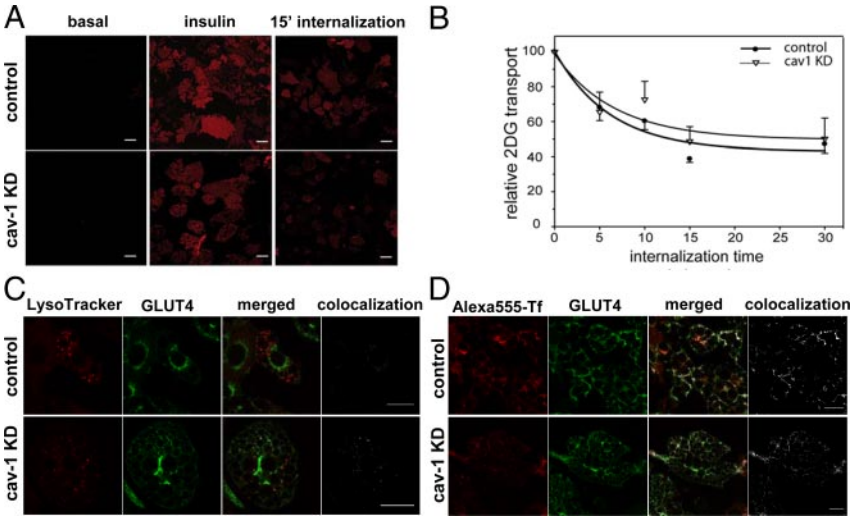

FIG. 6. GLUT4 internalization after insulin removal is not affected by caveolin-1 deficiency. A, PML were obtained from control and caveolin-1 KD adipocytes in the basal state, after 100 nM insulin treatment for 30 min, and 15 min after insulin washout. PML were stained with an anti-GLUT4 antibody. *Bar*, 25 μm. B, 2-Deoxyglucose (2DG) uptake was measured in control (●) and caveolin-1 KD (△) adipocytes after insulin removal at the time points indicated. For this, cells were first treated with 100 nM insulin for 30 min, washed twice with low pH KRM buffer [20 mM MES (pH 6.0), 120 mM NaCl, 5 mM KCl, 1.2 mM $MgSO_4$, 1.3 mM $CaCl_2$, 1.3 mM KH_2PO_4, 2 mM sodium pyruvate] to remove insulin and then incubated with 0.2% BSA-KRM (pH 6) buffer for the indicated times. Then the cells were washed with KRH buffer, and 2-deoxy-D-[1-^{3}H]glucose uptake was measured as described above. Serum-deprived control and caveolin-1 KD adipocytes were incubated with 50 nM LysoTracker Red (Molecular Probes) (C) or 1 μg/ml Alexa555-human transferrin (D) for 1 h at 37 C. Cells were then fixed, and GLUT4 was immunolocalized using OSCRX and a cyanine 5-conjugated secondary antibody. Quantitative colocalization analyses were performed using Huygens Essential software (IZASA SA). *Bar*, 25 μm.

formation that caveolae undergo when they are depleted of caveolin-1 and the implications of these.

Nevertheless, caveolin-1 absence has an important effect on adipocyte physiology. Caveolin-1-depleted preadipocytes become differentiated to adipocytes, but they show a considerable decrease in GLUT4 and IR protein expression, and this effect is due mainly to a reduction in the half-life of the transporter. The results suggest that most of the GLUT4 protein repression (but probably not the whole component) is explained by an enhanced rate of degradation. This observation suggests that caveolin-1/caveolae act as a stabilizer of GLUT4 and IR by preventing their degradation. We cannot exclude that caveolae structure or other components of caveolae, such as cavin, are responsible for these effects. Recently, Pilch's group (11) has shown that cavin KO mice, that lack caveolae in all cell types, also show a marked reduction of GLUT4 and IR expression in adipose tissue. In this cavin KO mouse, caveolin-1 expression is also decreased, the same as what happens when cavin expression is decreased in 3T3-L1 adipocytes (10). We have also found that caveolin-1 reduction leads to a decrease in cavin expression (data not shown). Thus, these results show that caveolae components are related.

Caveolin-1/caveolae could act as directing protein/organelle with a relevant role in determining the intracellular fate of IR and GLUT4. Caveolin-1/caveolae could favor intracellular recycling and prevent GLUT4 and IR degradation. Faster proteosome degradation of IR in adipose tissue has been previously described in caveolin-1 knockout mice (13). However, these mice present hyperinsulinemia and it has been largely documented that hyperinsulinemia can increase IR degradation (50–54). Nevertheless, caveolin-1 knockout mice show GLUT4 overexpression in adipose tissue (13). However, this effect could again be explained by long exposure to high levels of insulin, which have been described to stimulate GLUT4 expression (55–59). Liao's group has not described a decrease in GLUT4 and IR protein expression in their caveolin-1 KD 3T3-L1 adipocytes, however, they have performed their experiments with two monoclonal stably transfected cell lines (60, 61). Our data suggest that caveolin-1 reduction increases GLUT4 lysosomal degradation (Fig. 6C) and that this is independent of a differential distribution between endosomes and the insulin-responsive storage compartment (Fig. 6D). This observation points to an enhanced flux of GLUT4 from endosomes to lysosomes.

We have found that caveolin-1 KD in adipocytes causes a drop in GLUT4 and IR expression levels, and under these conditions, maximal insulin-stimulated glucose transport is markedly reduced, and insulin sensitivity is also diminished. It has previously been described that rat adipocytes with an 80% decrease in IR expression show a marked resistance to insulin, although maximal insulin response is preserved. These data are internally coherent provided that there are spare receptors in adipocytes (which also includes 3T3-L1 adipocytes), and therefore a decrease in IR reduces insulin sensitivity (62). In contrast, because of the central role of GLUT4 permitting an optimal insulin response, a reduction in GLUT4 impacts on maximal insulin-stimulated glucose transport (63).

Our results show that caveolae are not essential for GLUT4 internalization after insulin removal; however, caveolin-1 KD adipocytes show a 50% reduction in GLUT4 expression. Previously, by use of cholesterol-chelating agents, we and others have shown that integrity of lipid rafts is required for GLUT4 internalization (21, 23). Moreover, it has been shown that GLUT4 endocytosis in 3T3-L1 adipocytes is partially dependant on caveolae, using a dominant caveolin mutant (22) or in caveolin-1 KD adipocytes (61). Thus, we cannot discard a role of caveolae in GLUT4 internalization. In this regard, it may be helpful to examine rates of endocytosis or exocytosis to precisely characterize GLUT4 trafficking and to further address the effect of caveolin-1/caveolae in the time course and route of GLUT4 intracellular transit.

We consider that the increase in GLUT4 degradation can be explained in the absence of changes in GLUT4 internalization after insulin removal. Alternatively, GLUT4 degradation could be due to changes taking place under basal conditions because it has been described that the mechanisms for internalization and recycling differ in the basal state and after insulin removal (49,64,65).

Here we demonstrate that caveolin-1 deficiency in adipocytes has a direct effect on the expression of IR and GLUT4 proteins, independently of insulin levels, thereby demonstrating a main role of caveolin-1 in controlling the expression of proteins that are crucial in states of insulin resistance and obesity.

Acknowledgments

We thank Drs. D. Trono, A. Stahl, W. Stremmel, J. Peinado, and S. Jalkanen for the reagents, T. Yates for editorial support, Dr. Manel Bosch for his help in colocalization studies (Serveis Cientifico Tècnics, Universitat de Barcelona), and Francisco Simoes for technical assistance.

Address all correspondence and requests for reprints to: Marta Camps, Departament de Bioquímica i Biologia Molecular, Edifici Annex, Diagonal 645, 08028 Barcelona, Spain. E-mail: martacamps@ub.edu.

E.G.-M. was a Formación de Profesorado Universitario fellow from Ministerio de Educacion y Ciencia (MEC), Spain; M.C. was a Ramón y Cajal researcher from the MEC. This study was supported by research grants from the MEC (BMC2003-07279; BFU2006-13466/BMC; GEN2003-20662-C07), the Generalitat de Catalunya (2005SGR00947), and the Instituto de Salud Carlos III (Centro de Investigación Biomédica en Red de Diabetes y Enfermedades Metabólicas).

References

1. **Simons K, Ikonen E** 1997 Functional rafts in cell membranes. Nature 387: 569–572
2. **van Deurs B, Roepstorff K, Hommelgaard AM, Sandvig K** 2003 Caveolae: anchored, multifunctional platforms in the lipid ocean. Trends Cell Biol 13: 92–100
3. **Fan JY, Carpentier JL, van Obberghen E, Grunfeld C, Gorden P, Orci L** 1983 Morphological changes of the 3T3-L1 fibroblast plasma membrane upon differentiation to the adipocyte form. J Cell Sci 61:219–230
4. **Scherer PE, Lisanti MP, Baldini G, Sargiacomo M, Mastick CC, Lodish HF** 1994 Induction of caveolin during adipogenesis and association of GLUT4 with caveolin-rich vesicles. J Cell Biol 127:1233–1243
5. **Razani B, Combs TP, Wang XB, Frank PG, Park DS, Russell RG, Li M, Tang B, Jelicks LA, Scherer PE, Lisanti MP** 2002 Caveolin-1-deficient mice are lean, resistant to diet-induced obesity, and show hypertriglyceridemia with adipocyte abnormalities. J Biol Chem 277:8635–8647
6. **Cao H, Alston L, Ruschman J, Hegele RA** 2008 Heterozygous CAV1 frameshift mutations (MIM 601047) in patients with atypical partial lipodystrophy and hypertriglyceridemia. Lipids Health Dis 7:3
7. **Kim CA, DelépineM, Boutet E, El Mourabit H, Le Lay S, Meier M, Nemani M, Bridel E, Leite CC, Bertola DR, Semple RK, O'Rahilly S, Dugail I, Capeau J, Lathrop M, MagréJ** 2008 Association of a homozygous nonsense caveolin-1 mutation with Berardinelli-Seip congenital lipodystrophy. J Clin Endocrinol Metab 93:1129–1134
8. **Catalan V, Gomez-Ambrosi J, Rodriguez A, Silva C, Rotellar F, Gil MJ, Cienfuegos JA, Salvador J, Fruhbeck G** 2008 Expression of caveolin-1 in human adipose tissue is upregulated in obesity and obesity-associated type 2 diabetes mellitus and related to inflammation. Clin Endocrinol (Oxf) 68:213–219
9. **Hill MM, Bastiani M, Luetterforst R, Kirkham M, Kirkham A, Nixon SJ, Walser P, Abankwa D, Oorschot VM, Martin S, Hancock JF, Parton RG** 2008 PTRF-Cavin, a conserved cytoplasmic protein required for caveola formation and function. Cell 132:113–124
10. **Liu L, Pilch PF** 2008 A critical role of cavin (polymerase I and transcript release factor) in caveolae formation and organization. J Biol Chem 283:4314–4322
11. **Liu L, Brown D, McKee M, Lebrasseur NK, Yang D, Albrecht KH, Ravid K, Pilch PF** 2008 Deletion of Cavin/PTRF causes global loss of caveolae, dyslipidemia, and glucose intolerance. Cell Metab 8:310–317
12. **Cohen AW, Combs TP, Scherer PE, Lisanti MP** 2003 Role of caveolin and caveolae in insulin signaling and diabetes. Am J Physiol Endocrinol Metab 285:E1151–E1160
13. **Cohen AW, Razani B, Wang XB, Combs TP, Williams TM, Scherer PE, Lisanti MP** 2003 Caveolin-1-deficient mice show insulin resistance and defective insulin receptor protein expression in adipose tissue. Am J Physiol Cell Physiol 285:C222–C235
14. **Nystrom FH, Chen H, Cong LN, Li Y, Quon MJ** 1999 Caveolin-1 interacts with the insulin receptor and can differentially modulate insulin signaling in transfected Cos-7 cells and rat adipose cells. Mol Endocrinol 13:2013–2024
15. **Yamamoto M, Toya Y, Schwencke C, Lisanti MP, Myers Jr MG, Ishikawa Y** 1998 Caveolin is an activator of insulin receptor signaling. J Biol Chem 273: 26962–26968
16. **Baumann CA, Ribon V, Kanzaki M, Thurmond DC, Mora S, Shigematsu S, Bickel PE, Pessin JE, Saltiel AR** 2000 CAP defines a second signalling pathway required for insulin-stimulated glucose transport. Nature 407:202–207
17. **Gustavsson J, Parpal S, Karlsson M, Ramsing C, Thorn H, Borg M, Lindroth M, Peterson K H, Magnusson KE, StrâlforsP** 1999 Localization of the insulin receptor in caveolae of adipocyte plasma membrane. FASEB J 13:1961–1971
18. **Karlsson M, Thorn H, Parpal S, Strålfors P, Gustavsson J** 2002 Insulin induces translocation of glucose transporter GLUT4 to plasma membrane caveolae in adipocytes. FASEB J 16:249–251
19. **Parpal S, Karlsson M, Thorn H, Strålfors P** 2001 Cholesterol depletion disrupts caveolae and insulin receptor signaling for metabolic control via insulin receptor substrate-1, but not for mitogen-activated protein kinase control. J Biol Chem 276:9670–9678
20. **Robinson LJ, Pang S, Harris DS, Heuser J, James DE** 1992 Translocation of the glucose transporter (GLUT4) to the cell surface in permeabilized 3T3-L1 adipocytes: effects of ATP insulin, and GTPγS and localization of GLUT4 to clathrin lattices. J Cell Biol 117:1181–1196
21. **Ros-Baro A, Lopez-Iglesias C, Peiro S, Bellido D, Palacin M, Zorzano A, Camps M** 2001 Lipid rafts are required for GLUT4 internalization in adipose cells. Proc Natl Acad Sci USA 98:12050–12055
22. **Shigematsu S, Watson RT, Khan AH, Pessin JE** 2003 The adipocyte plasma membrane caveolin functional/structural organization is necessary for the efficient endocytosis of GLUT4. J Biol Chem 278:10683–10690
23. **Blot V, McGraw TE** 2006 GLUT4 is internalized by a cholesterol-dependent nystatin-sensitive mechanism inhibited by insulin. EMBO J 25:5648–5658
24. **Watson RT, Shigematsu S, Chiang SH, Mora S, Kanzaki M, Macara IG, Saltiel AR, Pessin JE** 2001 Lipid raft microdomain compartmentalization of TC10 is required for insulin signaling and GLUT4 translocation. J Cell Biol 154:829–840
25. **Chamberlain LH, Gould GW** 2002 The vesicle- and target-SNARE proteins that mediate Glut4 vesicle fusion are localized in detergent-insoluble lipid rafts present on distinct intracellular membranes. J Biol Chem 277:49750–49754
26. **Muñoz P, Mora S, Sevilla L, Kaliman P, Tomàs E, Gumà A, Testar X, Palacín M, Zorzano A** 1996 Expression and insulin-regulated distribution of caveolin in skeletal muscle. Caveolin does not colocalize with GLUT4 in intracellular membranes. J Biol Chem 271:8133–8139
27. **Frost SC, Lane MD** 1985 Evidence for the involvement of vicinal sulfhydryl groups in insulin-activated hexose transport by 3T3-L1 adipocytes. J Biol Chem 260:2646–2652
28. **Naldini L, BlömerU, Gage FH, Trono D, Verma IM** 1996 Efficient transfer, integration, and sustained long-term expression of the transgene in adult rat brains injected with a lentiviral vector. Proc Natl Acad Sci USA 93:11382–11388
29. **Brown DA, Rose JK** 1992 Sorting of GPI-anchored proteins to glycolipid-enriched membrane subdomains during transport to the apical cell surface. Cell 68:533–544
30. **Heuser JE, Anderson RG** 1989 Hypertonic media inhibit receptor-mediated endocytosis by blocking clathrin-coated pit formation. J Cell Biol 108:389–400
31. **Reid G, HübnerMR, Metivier R, Brand H, Denger S, Manu D, Beaudouin J, Ellenberg J, Gannon F** 2003 Cyclic, proteasome-mediated turnover of unliganded and liganded ERα on responsive promoters is an integral feature of estrogen signaling. Mol Cell 11:695–707
32. **Hansen JB, Petersen RK, Larsen BM, Bartkova J, Alsner J, Kristiansen K** 1999 Activation of peroxisome proliferator-activated receptor γ bypasses the function of the retinoblastoma protein in adipocyte differentiation. J Biol Chem 274:2386–2393
33. **Yang J, Clark AE, Kozka IJ, Cushman SW, Holman GD** 1992 Development of an intracellular pool of glucose transporters in 3T3-L1 cells. J Biol Chem 267:10393–10399
34. **Liu LB, Omata W, Kojima I, Shibata H** 2007 The SUMO conjugating enzyme Ubc9 is a regulator of GLUT4 turnover and targeting to the insulin-responsive storage compartment in 3T3-L1 adipocytes. Diabetes 56:1977–1985

35. **Biber JW, Lienhard GE** 1986 Isolation of vesicles containing insulin-responsive, intracellular glucose transporters from 3T3-L1 adipocytes. J Biol Chem 261:16180–16184
36. **Bach D, Naon D, Pich S, Soriano FX, Vega N, Rieusset J, Laville M, Guillet C, Boirie Y, Wallberg-Henriksson H, Manco M, Calvani M, Castagneto M, PalacínM, Mingrone G, Zierath JR, Vidal H, Zorzano A** 2005 Expression of Mfn2, the Charcot-Marie-Tooth neuropathy type 2A gene, in human skeletal muscle: effects of type 2 diabetes, obesity, weight loss, and the regulatory role of tumor necrosis factor α and interleukin-6. Diabetes 54:2685–2693
37. **Sargiacomo M, Sudol M, Tang Z, Lisanti MP** 1993 Signal transducing molecules and glycosyl-phosphatidylinositol-linked proteins form a caveolin-rich insoluble complex in MDCK cells. J Cell Biol 122:789–807
38. **Song KS, Li S, Okamoto T, Quilliam LA, Sargiacomo M, Lisanti MP** 1996 Co-purification and direct interaction of Ras with caveolin, an integral membrane protein of caveolae microdomains. Detergent-free purification of caveolae microdomains. J Biol Chem 271:9690–9697
39. **Drab M, Verkade P, Elger M, Kasper M, Lohn M, Lauterbach B, Menne J, Lindschau C, Mende F, Luft FC, Schedl A, Haller H, Kurzchalia TV** 2001 Loss of caveolae, vascular dysfunction, and pulmonary defects in caveolin-1 gene-disrupted mice. Science 293:2449–2452
40. **Razani B, Lisanti MP** 2001 Caveolin-deficient mice: insights into caveolar function human disease. J Clin Invest 108:1553–1561
41. **Farese RV** 2002 Function and dysfunction of αPKC isoforms for glucose transport in insulin-sensitive and insulin-resistant states. Am J Physiol Endocrinol Metab 283:E1–E11
42. **Welsh GI, Hers I, Berwick DC, Dell G, Wherlock M, Birkin R, Leney S, Tavaré JM** 2005 Role of protein kinase B in insulin-regulated glucose uptake. Biochem Soc Trans 33:346–349
43. **Chiang SH, Baumann CA, Kanzaki M, Thurmond DC, Watson RT, Neudauer CL, Macara IG, Pessin JE, Saltiel AR** 2001 Insulin-stimulated GLUT4 translocation requires the CAP-dependent activation of TC10. Nature 410:944–948
44. **Anderson RG** 1998 The caveolae membrane system. Annu Rev Biochem 67:199–225
45. **Parton RG** 1996 Caveolae and caveolins. Curr Opin Cell Biol 8:542–548
46. **Ostrom RS, Liu X** 2007 Detergent and detergent-free methods to define lipid rafts and caveolae. Methods Mol Biol 400:459–468
47. **Ring A, Le Lay S, Pohl J, Verkade P, Stremmel W** 2006 Caveolin-1 is required for fatty acid translocase (FAT/CD36) localization and function at the plasma membrane of mouse embryonic fibroblasts. Biochim Biophys Acta 1761:416–423
48. **Thomsen P, Roepstorff K, Stahlhut M, van Deurs B** 2002 Caveolae are highly immobile plasma membrane microdomains, which are not involved in constitutive endocytic trafficking. Mol Biol Cell 13:238–250
49. **Ishiki M, Klip A** 2005 Recent developments in the regulation of glucose transporter-4 traffic: new signals, locations, and partners. Endocrinology 146:5071–5078
50. **Krupp M, Lane MD** 1981 On the mechanism of ligand-induced down-regulation of insulin receptor level in the liver cell. J Biol Chem 256:1689–1694
51. **Green A, Olefsky JM** 1982 Evidence for insulin-induced internalization and degradation of insulin receptors in rat adipocytes. Proc Natl Acad Sci USA 79:427–431
52. **Ronnett GV, Knutson VP, Lane MD** 1982 Insulin-induced down-regulation of insulin receptors in 3T3-L1 adipocytes. Altered rate of receptor inactivation. J Biol Chem 257:4285–4291
53. **Heidenreich KA, Berhanu P, Brandenburg D, Olefsky JM** 1983 Degradation of insulin receptors in rat adipocytes. Diabetes 32:1001–1009
54. **Grako KA, Olefsky JM, McClain DA** 1992 Tyrosine kinase-defective insulin receptors undergo decreased endocytosis but do not affect internalization of normal endogenous insulin receptors. Endocrinology 130:3441–3452
55. **Yu ZW, Burén J, Enerbäck S, Nilsson E, Samuelsson L, Eriksson JW** 2001 Insulin can enhance GLUT4 gene expression in 3T3-F442A cells and this effect is mimicked by vanadate but counteracted by cAMP and high glucose: potential implications for insulin resistance. Biochim Biophys Acta 1535:174–185
56. **Olson AL, Pessin JE** 1995 Transcriptional regulation of the human GLUT4 gene promoter in diabetic transgenic mice. J Biol Chem 270:23491–23495
57. **Olson AL, Liu ML, Moye-Rowley WS, Buse JB, Bell GI, Pessin JE** 1993 Hormonal/metabolic regulation of the human GLUT4/muscle-fat facilitative glucose transporter gene in transgenic mice. J Biol Chem 268:9839–9846
58. **Charron MJ, Katz EB, Olson AL** 1999 GLUT4 gene regulation and manipulation. J Biol Chem 274:3253–3256
59. **Gerrits PM, Olson AL, Pessin JE** 1993 Regulation of the GLUT4/muscle-fat glucose transporter mRNA in adipose tissue of insulin-deficient diabetic rats. J Biol Chem 268:640–644
60. **Hong S, Huo H, Xu J, Liao K** 2004 Insulin-like growth factor-1 receptor signaling in 3T3-L1 adipocyte differentiation requires lipid rafts but not caveolae. Cell Death Differ 11:714–723
61. **Yuan T, Hong S, Yao Y, Liao K** 2007 Glut-4 is translocated to both caveolae and non-caveolar lipid rafts, but is partially internalized through caveolae in insulin-stimulated adipocytes. Cell Res 17:772–782
62. **Kono T, Barham FW** 1971 The relationship between the insulin-binding capacity of fat cells and the cellular response to insulin. Studies with intact and trypsin-treated fat cells. J Biol Chem 246:6210–6216
63. **Kahn BB, Simpson IA, Cushman SW** 1988 Divergent mechanisms for the insulin resistant and hyperresponsive glucose transport in adipose cells from fasted and refed rats. Alterations in both glucose transporter number and intrinsic activity. J Clin Invest 82:691–699
64. **Powell KA, Campbell LC, Tavare JM, Leader DP, Wakefield JA, Gould GW** 1999 Trafficking of Glut4-green fluorescent protein chimaeras in 3T3-L1 adipocytes suggests distinct internalization mechanisms regulating cell surface glut4 levels. Biochem J 344(Pt 2):535–543
65. **Dugani CB, Klip A** 2005 Glucose transporter 4: cycling, compartments and controversies. EMBO Rep 6:1137–1142